A continuation design framework for nonlinear flight control problems

T. S. Richardson, M. H. Lowenberg
Department of Aerospace Engineering
University of Bristol, UK

ABSTRACT

A methodology referred to as the continuation design framework is developed for application to nonlinear flight control problems. This forms the basis of a systematic approach to control system design for aircraft operating in highly nonlinear regions of the flight envelope. The essence of the continuation design framework is to combine bifurcation analysis with modern control methods such as eigenstructure assignment. Theoretical and practical issues of the approach are discussed with particular reference to the problems posed by agile fighter aircraft. The proposed methodology is applied to a fifth order hypothetical aircraft model and is shown to provide a visible, flexible and logical approach to nonlinear aircraft control law design.

NOMENCLATURE

Symbols

a	thrust model index
b	thrust model index
H	Height (m)
I_{xx}	moment of inertia about x-body axis
I_{xz}	product of inertia (x and z-body axes)
I_{yy}	moment of inertia about y-body axis
I_{zz}	moment of inertia about z-body axis
K_1^{fp}	thrust model coefficient
K_2^{fp}	thrust model coefficient
K_1^{mr}	thrust model coefficient
K_2^{mr}	thrust model coefficient
L	aerodynamic and propulsive rolling moment
M	aerodynamic and propulsive pitching moment or Mach number
N	aerodynamic and propulsive yawing moment
p	body axis roll rate
q	body axis pitch rate
r	body axis yaw rate
T	engine thrust
T_{fp}	full power thrust
T_{fp0}	full power thrust ($H = 0$, Mach number = 0)
T_{mr}	maximum reheat thrust
T_{mr0}	maximum reheat thrust ($H = 0$, Mach number = 0)
V_T	total translational velocity (constant)
$\mathbf{x}$	vector of n state variables
$\mathbf{x_d}$	desired system state
$\mathbf{x^*}$	equilibrium point
x_j	x-axis nozzle pivot displacement
y_j	y-axis nozzle pivot displacement
Y_w	y-wind axis aerodynamic forces
z_j	z-axis nozzle pivot displacement
Z_w	z-wind axis aerodynamic forces

Paper No. 2949. Manuscript received 22 December 2004, revised version received 5 September 2005, accepted 12 October 2005.

https://doi.org/10.1017/S0001924000001032 Published online by Cambridge University Press

Abbreviations

BA	bifurcation analysis
BACTM	bifurcation and catastrophe theory methodology
CDF	continuation design framework
EA	eigenstructure assignment
HHIRM	hypothetical high incidence research model
ICE	innovative control effectors
LQR	linear quadratic regulator
UCAV	uninhabited combat air vehicle

Greek letters

α	angle-of-attack
β	angle-of-sideslip
$\boldsymbol{\delta}$	vector of m controls
δ_a	aileron deflection (degrees)
δ_e	elevator deflection (degrees)
δ_r	rudder deflection (degrees)
δ_{roll}	thrust vectoring roll control deflection (degrees)
δ_t	throttle control input – $0 \le \delta_t \le 1{\cdot}0$
δ_{tfp}	full power throttle control input
δ_{yaw}	thrust vectoring yaw control deflection (degrees)
λ	continuation parameter
ρ	density

1.0 INTRODUCTION

The continuation design framework (CDF) is a practical extension to the bifurcation analysis and catastrophe theory methodology (BACTM) laid out by Mehra *et al*[1-3]. It provides a novel and comprehensive approach to the control of highly nonlinear systems, with particular application to aircraft flight dynamics problems. A particular strength of the CDF is that the combination of analysis and design methodologies leads to a much greater insight and understanding of both the open and closed loop systems. This paper demonstrates advantages of the CDF approach, especially when employed for rapid control law prototyping.

Bifurcation analysis is a methodology whereby a map of fixed points (steady states) in state/parameter space is generated for a nonlinear system. The stability of branches of these fixed points can be examined in light of nonlinear systems theory, enabling the global nonlinear behaviour of the system to be inferred. The CDF extends this in an inverse sense, facilitating the design of the system to meet desired behaviour. In principle, this can be applied to optimise airframe sizing to meet stability and control requirments; but in practise, by the time a good nonlinear mathematical model of aerodynamic reactions has been derived, the airframe shape and size is generally frozen. In practice therefore, the CDF is more useful for control law design.

In this paper the open loop nonlinear system topology of a theoretical aircraft model, the hypothetical high incidence research model (or HHIRM) is examined. Strategies for control are derived, and subsequent control system design is carried out using the CDF. A fifth order version of the HHIRM is implemented and substantial improvement in the aircraft response is demonstrated. Control system design is carried out in accordance with desired handling qualities levels.

The paper is organized as follows. The problem definition and proposed continuation design framework is presented in Section 2. Section 3 outlines the underlying theory contained within the framework. The HHIRM is presented in Section 4 and the open loop aircraft analysis in Section 5. Section 6 contains results for the closed loop augmented HHIRM. Conclusions are given in Section 7.

1.1 Problem definition

Research conducted in the late 1970s (Mehra *et al*[1-3]) demonstrated the first comprehensive application of bifurcation analysis methods to the flight dynamics field. The work carried out by Mehra during this three year period was extensive and touched on many areas of interest that are still under consideration today. Bifurcation analysis and catastrophe theory methodology, as the new technique was named, was applied to several different fighter aircraft models. Results were generated for specific examples that related to jump, hysteresis and limit cycle phenomena. A clear demonstration of the new method's potential was the identification for the first time of wing rock onset as a Hopf bifurcation and its development into a stable limit cycle.

The vast majority of subsequent applications of bifurcation analysis dealt with the assessment of existing open loop and closed loop systems, e.g. Jahnke[4,5], Guicheteau[6], Liebst and Planeaux[7], Lowenberg[8-11], etc. Some of this work focussed on the assessment of new control laws, e.g. Littleboy, Nichols & Gibson[12] and Littleboy and Smith[13], but the methodology had not been extended to enable it to contribute directly to the controller design process. Lowenberg[8] initiated this in the context of feedforward systems and the development of bifurcation tailoring which is the manipulation of the fixed point maps in state-parameter space. Both Mehra and Lowenberg used open loop control in the form of aileron-rudder interconnects to provide bifurcation-free manoeuvres.

The CDF however deals with feedback systems, allowing bifurcation tailoring to address both the stability and handling qualities requirements of highly nonlinear aircraft models with wide operating envelopes. The CDF approach combines continuation methods with control system design processes. In this paper the control systems design is achieved within the CDF using a classical state feedback control structure and eigenstructure assignment embedded within the continuation algorithm.

1.2 Continuation design framework

A summary of the CDF methodology follows. As this is an extension to the BACTM methodology, it involves steps identified by Mehra[1-3], Goman[14-16] and Lowenberg[8]. The novel additional steps are related to the explicit integration of a controller design method and implementation in the context of design rather than for assessment only. The framework has been laid out in three sections which relate to the baseline analysis, checking the feasibility of the desired equilibria, and control system design.

Note: not all these steps will always be necessary and individual steps may be omitted depending on the design problem being addressed.

A – Analysis of the baseline model

1. Creation of one-parameter bifurcation diagrams for the baseline nominal system.
2. Calculation of asymptotic stability regions for all the discovered attractors (equilibria/fixed points and, in general, closed orbits).
3. Examination of eigenstructure variation (eigenvalues and eigenvectors).
4. Prediction of aircraft behaviour using information about the evolution of the phase portrait and eigenstructure with the continuation parameters.
5. Use of time histories to check the predicted behaviour and transient characteristics of the aircraft.

B – Define and check feasibility of desired equilibria

6. Identify desired change in operating characteristics, specify design goal in terms of the equilibria and eigenstructure.
7. Identify if the design goal is achievable physically and if a possible steady state solution exists;

https://doi.org/10.1017/S0001924000001032 Published online by Cambridge University Press

i.e. use an inverse approach: find the parameter values (control surfaces) that are required to give the desired branch of equilibria. The desired equilibria will only exist if there is sufficient control power available.

C – Design and evaluate gain scheduled controller

8. Select a suitable controller structure and control algorithm e.g. state feedback or PID, LQR or eigenstructure assignment.
9. Implement controller structure and solve iteratively during continuation for the controller gains (taking care to extract the correct local stability for the desired branch).
10. If necessary re-run the continuation solving for additional branches, revealing the global structure of the closed loop system with the gains determined in step 9.
11. Use appropriate transformations to create state scheduled dynamic controllers from the closed loop variation in gain. This will account for hidden coupling terms when scheduling gains against closely coupled states.
12. Use of time histories to check the predictions and transient characteristics of the closed loop aircraft.

2.0 NOTES ON THE FRAMEWORK

The result of these steps is a methodology that, whilst requiring knowledge of nonlinear systems theory, provides a much deeper understanding of both the open and closed loop systems than conventional approaches. The CDF formalises and extends conventional control systems design approaches based on gridding, trimming and linearisation of nonlinear aircraft models.

The use of eigenstructure assignment allows the placement of selected eigenvalues with the use of selected state feedback. Integration of the eigenstructure assignment algorithm within the continuation algorithm allows elements of the controller to be scheduled with outputs, states and/or parameters. For example, eigenvalue position could be linked to chosen aircraft states and eigenvector requirements could be relaxed at high angles of attack. Integration of the gain calculation within the continuation algorithm also ensures that the aircraft plus controller states are in trim at each solution point.

Other methods for gain calculation can easily be implemented in place of Eigenstructure Assignment and current work in Bristol includes the application of LQR[17] within the CDF framework to the ICE[18] (innovative control effectors) UCAV model.

Continuation methods are based on steady states so numerical simulation is necessary to check the predictions and transient characteristics of the aircraft for large amplitude and/or rapid state and parameter disturbance. The faster the parameter changes, the greater the difference between the steady-state solution and transient motion.

Gain variation may be highly nonlinear and implemented schedules may have to be simplified. The gains are calculated during each iteration and are stored for each solution point. As such, the resulting gains show smooth variation with the states x but the desired stability of the system is only achieved for fixed gains around any given equilibrium point $\mathbf{x}^*$.

These gains can either be scheduled against the continuation parameter (e.g. stick position) and/or uncoupled states. Alternatively the gain variations can be transformed and scheduled against desired system states $\mathbf{x_d}$[19,20]. The resultant controller allows rapid variation in the scheduled variable whilst ensuring that the system response closely tracks the desired response for each instantaneous state of the system.

The continuation design framework allows a more subtle approach to control system design. Analysis of the baseline aircraft model within the framework allows regions to be selected within which the dynamic response is unacceptable. Within these regions closed loop and feedforward control is used to modify the individual aircraft modes in light of existing control power. For example, where aerodynamic controls lose authority at high angles of attack, either the design requirements can be relaxed and/or additional control motivators may be introduced.

3.0 THEORETICAL BACKGROUND

3.1 Bifurcation analysis

Bifurcation analysis for dynamical systems is normally applied to a nonlinear model expressed as n first order autonomous differential equations:

$$\dot{\mathbf{x}} = \boldsymbol{f}(\mathbf{x},\boldsymbol{\delta}) \qquad \mathbf{x}, \boldsymbol{f} \in \Re^n \qquad \boldsymbol{\delta} \in \Re^m \qquad \ldots (1)$$

where $\mathbf{x}$ is a vector of n state variables
$\boldsymbol{\delta}$ is a vector of m controls
$\dot{\mathbf{x}}$ is the time derivative of x
$\boldsymbol{f}$: $\Re^n \times \Re^m \rightarrow \Re^n$ is the continuous vector field (the n nonlinear functions)

In the aircraft case, $\boldsymbol{f}$ consists of the standard flight dynamics equations of motion; when feedback controllers are incorporated in the model then equations are added to describe control, actuator and sensor dynamics.

The basis of bifurcation analysis applied to large-scale highly nonlinear models, such as aircraft, is the calculation of fixed points (which are also referred to as zeroes, equilibria or stationary solutions) i.e. $\dot{\mathbf{x}} = 0$. A full analysis often involves generating paths of periodic orbit solutions in additional to those of the fixed points; these are not required for the purposes of this paper. In this paper, branches of fixed points are found as a selected parameter varies whilst the other input values remain constant. The parameter selected for this purpose is known as the continuation parameter, λ (a member of the parameter vector, $\boldsymbol{\delta}$). A numerical continuation algorithm is used to solve for branches of steady states as λ is varied, with equilibrium specified as:

$$\dot{\mathbf{x}} = \boldsymbol{f}(\mathbf{x}, \lambda) = 0 \qquad \mathbf{x}, \boldsymbol{f} \in \Re^n \qquad \lambda \in \Re \qquad \ldots (2)$$

Continuation methods rely upon the implicit function theorem, which states that if the Jacobian matrix of the linearised system at a fixed point is invertible (i.e. non-singular) then there exists locally a unique solution. So for all fixed points excluding those with a real eigenvalue lying at zero, there exists locally a unique fixed point for the given value of λ. Therefore for a smooth variation in λ from an initial fixed point there must exist a unique curve of fixed points. This assumes that the Jacobian remains non-singular; but most continuation methods possess the ability to solve through certain classes of singularity, e.g. folds (using the properties of an 'extended' Jacobian).

As parameters vary in a dynamical system, changes may occur in the qualitative structure of the dynamics at certain parameter values. These changes are called bifurcations and the corresponding state/parameter values, bifurcation points. There are various types of bifurcations, classified according to the centre manifold and other dynamical systems theorems (see, for example, Ref. 21).

The continuation algorithm solves for the branch using a predictor-corrector method. If an initial solution is known, then the system can be extrapolated in the local region by an incremental approximation in each system state Δx_i. Newton's method[22] is then used to reduce the error between the approximation and the new fixed point. For a continuous system, the fixed-point solution path can be determined across the selected range of the continuation parameter values.

https://doi.org/10.1017/S0001924000001032 Published online by Cambridge University Press

Table 1
Bifurcation diagram notation

Line type	Equilibria type
Solid	Stable
Dashed	Unstable (divergent)
Dotted	Unstable (oscillatory)

In order to generate all the branches that are present within a given parameter range, a set of starting solutions is required for the system. One of the main difficulties in applying bifurcation methods is in finding these initial solutions. There are several approaches to solving this problem, some systematic, some that require flight dynamics insight and some based on the nonlinear systems theory. It should be noted, however, that none of the methods can be guaranteed to find all the starting solutions for a given set of nonlinear equations. In most cases though, a combination of methods and perseverance allows a comprehensive set of starting solutions to be found.

As the continuation along the branch proceeds, the system is linearised about each fixed point in order to investigate its local properties. The theorem attributed to Liapunov (1892)[23] relates the stability of a nonlinear system to eigenvalues, μ_j, of the linearised system, i.e of the Jacobian evaluated at the stationary point:
$\mathrm{Re}(\mu_j) < 0$ for all j implies asymptotic stability
$\mathrm{Re}(\mu_k) > 0$ for one (or more) k implies instability of some kind

Results are usually presented in the form of one-parameter bifurcation diagrams showing each individual system state component solution versus the continuation parameter. The stability of each branch is indicated by line type. The conventions used in this paper are shown in Table 1. Since limit cycles are not investigated here the only bifurcation results presented are those relating to system equilibria.

Linearisation and stability analysis of a nonlinear system can be carried out at any point and simply indicates the behaviour of the system as if it were trimmed about that point. Evaluating the continuous set of fixed points of a nonlinear system instead of simply gridding the flight envelope has several major advantages. It results in a more feasible problem (reduced number of points to examine) and may be more easily interpreted (e.g. a fixed point at low a may correspond to conventional trimmed flight of the aircraft) and these steady state conditions govern the way in which transient response develops. Examination of the parameter dependence of the fixed points using continuation methods and bifurcation theory will also take into account nonlinear effects present in the system. Control surface saturation for example can be easily identified together with the steady-state deflections required for trimmed flight.

3.2 System stability

In the normal application of bifurcation analysis to a system, the same set of equations is used for both continuation and when linearising the system to evaluate the system stability. The continuation design framework however incorporates several steps where the system being used for continuation could be different to that used for the stability analysis.

For example, in this paper, when using the continuation algorithm to calculate steady state control deflections for given aircraft states two different systems are used. In the first, the control deflections (states) are found whilst trimming a constrained set of aircraft equations of motion. In the second, the control surface deflections are fixed and the system linearised with respect to the aircraft states in order to find the correct Jacobian and corresponding stability.

There are other instances where it is useful to be able to distinguish between the system being used for continuation and the system used for stability analysis at each fixed point. Equations (3) and (4) represent two nonlinear systems. In the general case, these two systems need not be related but for most practical aircraft applications they are linked in some way, usually via the aircraft equations of motion with different constraint equations.

$$\dot{\mathbf{x}}_1 = \boldsymbol{f}_1(\mathbf{x}_1, \boldsymbol{\delta}_1) = 0 \qquad \mathbf{x}_1, \boldsymbol{f}_1 \in \Re^n \qquad \boldsymbol{\delta}_1 \in \Re^m \qquad \ldots (3)$$

$$\dot{\mathbf{x}}_2 = \boldsymbol{f}_2(\mathbf{x}_2, \boldsymbol{\delta}_2) = 0 \qquad \mathbf{x}_2, \boldsymbol{f}_2 \in \Re^i \qquad \boldsymbol{\delta}_2 \in \Re^k \qquad \ldots (4)$$

Two general examples of where two systems might be used in the CDF methodology are when solving for algebraic constraints on the aircraft (e.g. when using a specific steady or quasi-steady state condition such as turning flight) and when solving for gain schedules during a continuation run. In a more general design application, where optimisation is performed on a set of parameters to meet several separate design criteria, more than two models may be used.

4.0 AIRCRAFT MODEL – HHIRM

The Hypothetical High Incidence Research Model (HHIRM)[24], was created to provide a benchmark for nonlinear analysis and control design. It was developed by Goman, Khramtsovsky and Usoltsev in 1995 for the then UK Defense Research Agency (now QinetiQ). The aerodynamic characteristics of the HHIRM are very similar to those of many existing combat aircraft and can be easily tuned to arbitrarily chosen characteristics for qualitative nonlinear dynamics analysis and control law design.

The HHIRM is ideal for research into control law design because the aerodynamic and thrust models are entirely based upon simple mathematical functions of aircraft parameters. The aerodynamic control surfaces used in this work are the elevator ($-40 \le \delta_e \le 40$ degrees), aileron ($-30 \le \delta_a \le 30$ degrees) and rudder ($-30 \le \delta_r \le 30$ degrees). No control surface rate limits are applied. All the functions used to create the aerodynamic model are smooth, and it is therefore implicit that within the specified control surface limits the model may be highly nonlinear but remains smooth (differentiable) with continuous first derivatives. The use of mathematical functions instead of large unwieldy aerodynamic tables means that the software code for the entire model is far smaller and faster to run.

In the asymmetric version of the model, lateral-directional asymmetry appears at zero sideslip, zero rotation rate and zero aileron and rudder deflection above a certain angle-of-attack, α. This is uncontrollable at very high α using rudder and aileron due to both reduced control surface authority and large lateral-directional moments. There is also an associated loss of directional stability due to shadowing of the vertical tail, and loss of lateral stability arising from forebody vortex breakdown effects. In this paper we consider the fifth order reduced-order form of the model.

4.1 Fifth order HHIRM

The fifth order implementation of the HHIRM represents the approximate short period, Dutch roll and roll subsidence modes:

$$\begin{aligned}
\dot{\alpha} &= q - \mathrm{Tan}\beta(p\mathrm{Cos}\alpha + r\mathrm{Sin}\alpha) + \frac{Z_W}{mV_T\mathrm{Cos}\beta} \\
\dot{\beta} &= p\mathrm{Sin}\alpha - r\mathrm{Cos}\alpha + \frac{Y_W}{mV_T} \\
\dot{p} &= \frac{1}{I_{xx}}\left[\left(I_{yy} - I_{zz}\right)qr + I_{xz}\left(\dot{r} + pq\right) + L\right] \\
\dot{q} &= \frac{1}{I_{yy}}\left[\left(I_{zz} - I_{xx}\right)rp + I_{xz}\left(r^2 - p^2\right) + M\right] \\
\dot{r} &= \frac{1}{I_{zz}}\left[\left(I_{xx} - I_{yy}\right)pq + I_{xz}\left(\dot{p} - qr\right) + N\right]
\end{aligned} \qquad \ldots (5)$$

https://doi.org/10.1017/S0001924000001032 Published online by Cambridge University Press

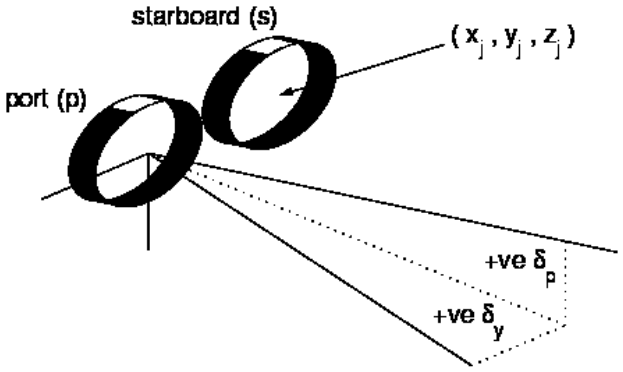


Figure 1. Thrust vector alignment.

A complete breakdown of the aerodynamic model is given in Ref. 24. In summary however, the force and moment terms (Y_w, Z_w, L, M and N) include both aerodynamic and propulsive components calculated using the predefined mathematical functions.

4.2 HHIRM thrust model

The HHIRM includes a nonlinear engine model, as well as thrust vectoring for use in advanced control law design. There have been several notable research programmes (e.g. NASA F-18 HARV[25]) where thrust vectoring has been shown to dramatically improve aircraft handling in the high α regions of the flight envelope.

The HHIRM is considered to be a twin engine aircraft with the subscripts s and p in the following equations denoting the starboard and port engines respectively. Full power (T_{fp}) and maximum reheat (T_{mr}) thrust are approximated for any given point in the flight envelope as follows:

$$T_{fp} = T_{fp0}\left(1 + K_1^{fp}(H)M + K_2^{fp}(H)M^2\right)\left(\frac{\rho(H)}{\rho(0)}\right)^a \quad \ldots (6)$$

$$T_{mr} = T_{mr0}\left(1 + K_1^{mr}(H)M + K_2^{mr}(H)M^2\right)\left(\frac{\rho(H)}{\rho(0)}\right)^b \quad \ldots (7)$$

The coefficients K_1^{fp}, K_2^{fp}, K_1^{mr}, K_2^{mr} and a and b are calculated using the same spline routines that are used for the aerodynamic data. Full power thrust T_{fp0} ($H = 0$, $M = 0$) and maximum reheat thrust T_{mr0} ($H = 0$, $M = 0$) are constants.

A simple linear interpolation is then used to calculate the power produced at the current throttle setting δ_t. Equation (8) is used when the throttle setting $\delta_t < \delta_{tfp}$ and Equation (9) when the throttle setting δ_t is in the reheat region.

$$T = T_{fp}\frac{\delta_t}{\delta_{t_{fp}}} \quad \ldots (8)$$

$$T = T_{fp} + (T_{mr} - T_{fp})\frac{\delta_t - \delta_{tfp}}{1 - \delta_{tfp}} \quad \ldots (9)$$

Thrust vectoring is considered to be obtainable in two axes for each nozzle independently. The direction of thrust is controlled with parameters δ_p and δ_y corresponding to nozzle deflection. These are shown in Fig. 1 applied to the port nozzle (p). Note the central line corresponds to the engine axis which is aligned to the body axis of the aircraft. The thrust vectoring is applied in order to increase the available control power, in particular in the high alpha regions of the flight envelope where the aerodynamic control surfaces lose authority.

Positions of the starboard and port nozzle hinges as shown in Fig. 1 are given in Equations (10) and (11) (metres). The only difference between the two nozzle positions is a lateral displacement. This is symmetric around the centreline which is indicated by the displacement being at $\pm y_j$.

$$\mathbf{r_s} = (x_j, y_j, z_j) = (5{\cdot}0,\ 0{\cdot}5,\ 0{\cdot}0) \quad \ldots (10)$$

$$\mathbf{r_p} = (x_j, -y_j, z_j) = (5{\cdot}0,\ -0{\cdot}5,\ 0{\cdot}0) \quad \ldots (11)$$

Several assumptions are made in order to simplify the engine model. The first is that the throttle setting to each nozzle is identical, resulting in a single throttle control. The second is that the deflection of each nozzle is coupled to the other. Simultaneous deflection of the nozzles laterally (δ_y) in the same sense allows a contribution to yaw control. Differential deflection in pitch (δ_p) with the deflection of each nozzle being directly proportional but in an opposite sense allows a contribution to roll control. Thus nozzle deflection is linked to two new control variables δ_{roll} and δ_{yaw}. It is assumed that the nozzles are ideal and therefore there are no thrust losses associated with nozzle vectoring. A maximum nozzle deflection of ±20 degrees is used in this paper.

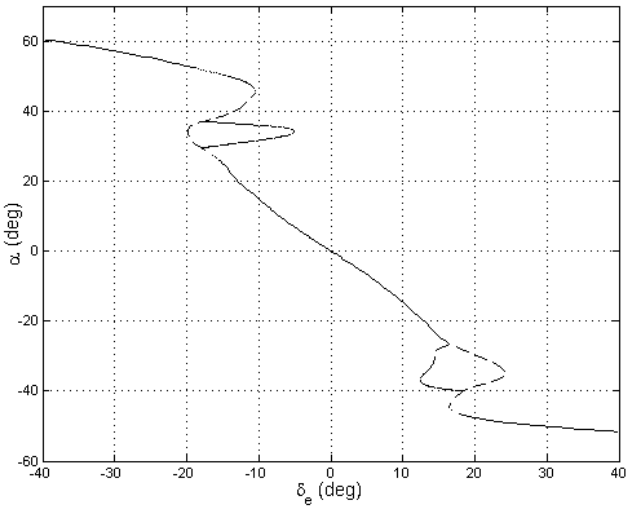


Figure 2. α (deg) *vs* δ_e (deg) for the symmetric HHIRM.

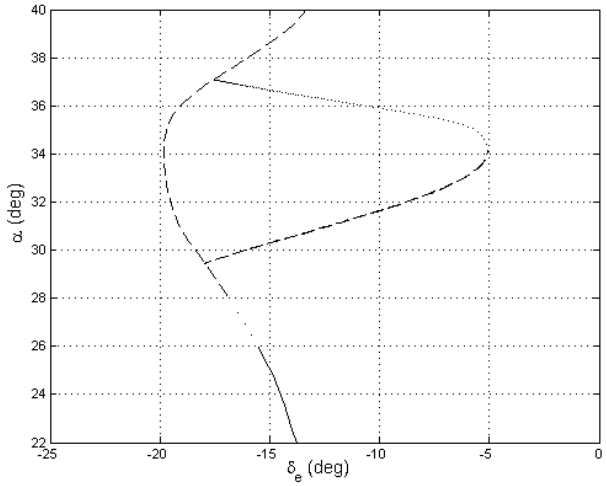


Figure 3. α (deg) *vs* δ_e (deg) reduced range for the symmetric HHIRM.

https://doi.org/10.1017/S0001924000001032 Published online by Cambridge University Press

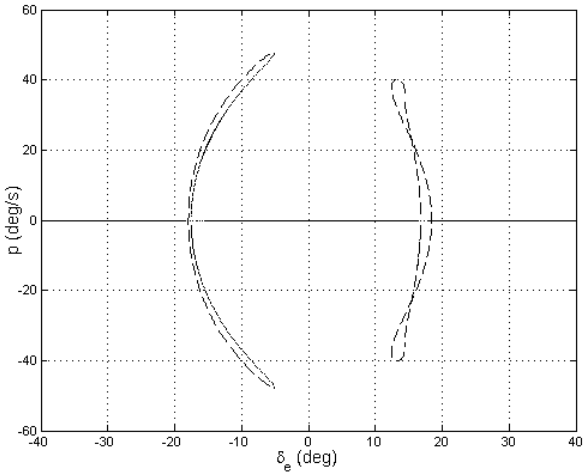


Figure 4. *p* (deg/s) *vs* δ_e (deg) for the symmetric HHIRM.

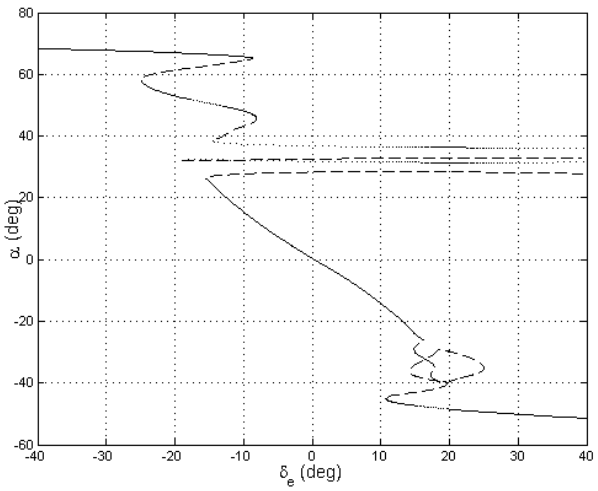


Figure 5. α (deg) *vs* δ_e (deg) for the asymmetric HHIRM.

5.0 HHIRM BASELINE

5.1 Symmetric fifth order HHIRM

The results given in this section are for the nominal baseline HHIRM configuration. Figures 2, 3 and 4 are bifurcation diagrams of α and p plotted against the continuation parameter, δ_e. Three branches are shown in each plot: the main trim branch, which exists with zero lateral-directional variables between $\delta_e = \pm 40$ degrees; and two unstable spin branches which intersect with the main trim branch. All branches are symmetric about zero for the lateral states. At low α the main trim branch is stable, corresponding to conventional flight at low angles-of-attack.

In Figs 2 and 3 at $\alpha = 26.5$ degrees there is a qualitative change in stability from stable to oscillatory unstable with a complex conjugate pair of eigenvalues crossing through the imaginary axis indicating a Hopf bifurcation. This corresponds to the Dutch roll mode going unstable and relates to the possible onset of wing rock. It is not possible to tell from the fixed points whether a stable limit cycle is created (limit cycles would need to be solved for separately). This section of the equilibria branch does not exist over a wide parameter range and at 28 degrees α there is another change in stability from oscillatory unstable to divergent behaviour. This relates to the complex pair in the right half plane meeting on the real axis and separating into two real eigenvalues. The system then remains unstable up to $\alpha = 45{\cdot}5$ degrees where the branch again becomes oscillatory unstable. This continues until a second Hopf bifurcation at $\alpha = 52{\cdot}3$ degrees. The remaining section of the branch (deep stall, down to –40 degrees elevator and $\alpha = 60{\cdot}5$ degrees) is stable.

The two symmetric branches with non-zero roll rate, p, that exist at large negative and positive α both cross the main branch at pitchfork bifurcations. As both of these branches are unstable they do not represent stable attractors towards which a trajectory would move but would interact with the main branch to produce highly nonlinear behaviour. For example, there is a section of the plot relating to a fixed elevator deflection for which there is no stable branch. At this point the aircraft could either move towards a stable limit cycle or enter oscillatory (possibly chaotic) behaviour governed by the multiple branches that exist for that elevator deflection.

At this point results have been generated which correspond to CDF steps 1 (creation of one-parameter bifurcation diagrams) and 4 (prediction of aircraft behaviour) in the analysis of the baseline model. It is possible to look more closely at the eigenvalue variation, estimate basins of attraction and generate time simulations; here however, we move on to a second set of results for the asymmetric model which represents a second challenging control problem.

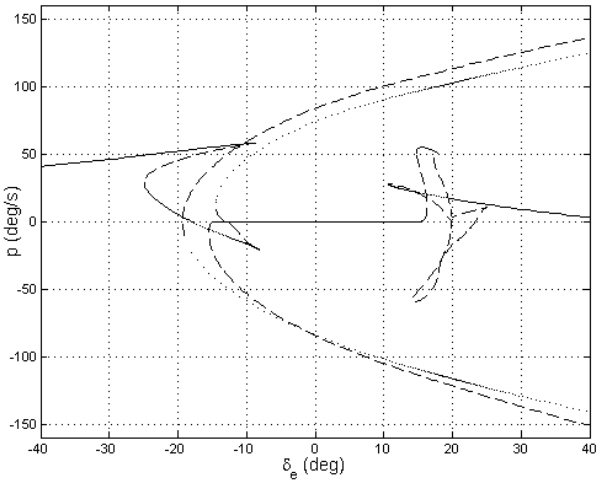


Figure 6. *p* (deg/s) *vs* δ_e (deg) for the asymmetric HHIRM.

5.2 Asymmetric fifth order HHIRM

Figures 5 and 6 contain the bifurcation diagrams for the fifth order asymmetric HHIRM. As before, two of the five states are shown, α and p, plotted against the continuation parameter δ_e. As expected, the plots are no longer symmetric with asymmetric lateral-directional components arising in all three branches. In the low α region however, the main trim branch is symmetric, consistent with conventional low α flight. The modes in this region are decoupled and relatively well damped which would be reflected in the eigenvalues and eigenvectors of the system if linearised in this region.

https://doi.org/10.1017/S0001924000001032 Published online by Cambridge University Press

As α increases, asymmetry sets in at approximately 26 degrees α and the system folds very shortly afterwards undergoing a change in stability corresponding to a single real eigenvalue crossing into the right half plane. The limit of this branch is at the maximum positive elevator deflection, (δ_e = +40 degrees).

The upper branch appears similar in nature to the symmetric implementation with a stable deep stall although the branch now has nonzero lateral components. As it folds back down to lower α, there are associated changes in stability. The limits on both the upper and mid branches are linked to the maximum elevator deflection.

As with the symmetric HHIRM model one-parameter bifurcation diagrams have been generated. In the next two sections, steps 6 and 7 of the CDF are considered; identify the desired change in operating characteristics and identify if the design goal is physically achievable.

5.3 Open loop bifurcation tailoring of equilibria

One way of checking whether the design goal is physically achievable, (i.e. that it is possible to create the desired steady state) is to carry out an implicit inversion of the state equations in order to obtain the desired steady state point or branch. This is achieved through the open loop bifurcation tailoring of the system, where the continuation algorithm is used to find control surface deflections consistent with desired steady states. The calculation of steady state control deflections or parameters will allow demanded trim conditions to be defined but will not guarantee or specify the associated stability. Consider a system described by:

$$\dot{\mathbf{x}} = \boldsymbol{f}(\mathbf{x}, p, \mathbf{q}) \quad \ldots (12)$$

$$\mathbf{y} = \mathbf{h}(\mathbf{x}) \quad \ldots (13)$$

where
$\mathbf{x} \in \Re^n$ system state,
$p \in \Re^l$ is a slow-varying system input,
$\mathbf{y} \in \Re^m$ system output and
$\mathbf{q} \in \Re^m$ is the vector of all system inputs other than p

The bifurcation tailoring problem[8,26] is to design a control law $\mathbf{q}$ such that the output of the controlled system has a desired dynamical behaviour as the parameter p varies from p_a to p_b:

$$y_d^*(p) = \mathbf{g}(p, t) \qquad \text{for } p \in [p_a, p_b] \quad \ldots (14)$$

where for a given $p \in [p_a , p_b]$, $\mathbf{g}(p, t)$ could be a point, a limit cycle or even chaotic. In order to check the feasibility of a desired steady state, only the bifurcation tailoring of equilibria is considered. Without loss of generality, we could assume that the outputs are the first m states of the system which we label $\mathbf{x_I}$

$$\mathbf{y} = \mathbf{x_I} = [x_1, \ldots, x_m]^T \quad \ldots (15)$$

In what follows we focus our attention on the problem where the desired objective is for the controlled system to exhibit a branch of equilibria such that, as the parameter p is varied:

$$\mathbf{x_I}(p) = \mathbf{g}(p) \qquad \text{for } p \in [p_a, p_b] \quad \ldots (16)$$

where $\mathbf{g}$ is an m-dimensional smooth function of p. This means that, for a given $p \in [p_a, p_b]$, the desired output is a point, and that this point varies smoothly as p varies from p_a to p_b. Partition the state vector $\mathbf{x}$ as $\mathbf{x} = [\mathbf{x_I}^T \ \mathbf{x_{II}}^T]^T$ where $x_{II} = [x_{m+1} \ldots x_n]^T$ and define the auxiliary vector $\mathbf{z}$ as:

$$\mathbf{z} = \begin{bmatrix} \boldsymbol{x}_{II} \\ \boldsymbol{q} \end{bmatrix} \quad \ldots (17)$$

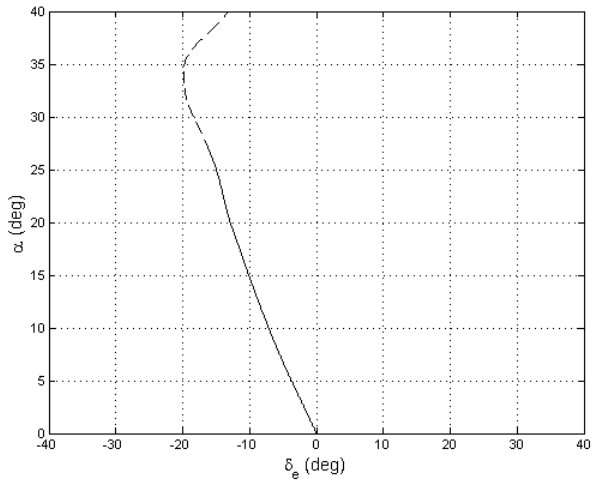


Figure 7. α (deg) *vs* δ_e (deg) for the asymmetric HHIRM tailored to give $\beta = p = 0$.

For any given $p \in [p_a, p_b]$, $z \in \Re^n$ should satisfy the equation:

$$\boldsymbol{f}(\boldsymbol{g}(p), \boldsymbol{x}_{II}, p, \boldsymbol{q}) \equiv \tilde{\boldsymbol{f}}(\boldsymbol{z}, p) = 0 \quad \ldots (18)$$

In fact, if Equation (18) is satisfied, the system will exhibit a branch of equilibria with the desired shape over the parameter range $p \in [p_a, p_b]$. The implicit function theorem states that if the Jacobian of $\mathbf{f}$ with respect to $\mathbf{z}$ is invertible, then Equation (18) implicitly defines $\mathbf{z}$ as a function of p, i.e.

$$\mathbf{z} = \boldsymbol{z}_d^*(p) = \begin{bmatrix} \boldsymbol{x}_{IId}^*(p) \\ \boldsymbol{q}_d^*(p) \end{bmatrix} \quad \ldots (19)$$

which means that

$$\mathbf{x}_\mathbf{d}^* = \begin{bmatrix} \boldsymbol{x}_{Id}^*(p) \\ \boldsymbol{x}_{IId}^*(p) \end{bmatrix} \quad \ldots (20)$$

is an equilibrium point of the open loop system

$$\dot{\mathbf{x}} = \mathbf{f}(\mathbf{x}, p, \mathbf{q}_\mathbf{d}^*(p)) \quad \ldots (21)$$

Therefore, if $\mathbf{x}_\mathbf{d}^*$ is an asymptotically stable equilibrium point of Equation (21) for any $p \in [p_a, p_b]$, then it is possible to use the control input $\mathbf{q} = \mathbf{q}_\mathbf{d}^*(p)$ to generate the desired steady states:

$$\mathbf{z} = \boldsymbol{z}_d^*(p_a) = \begin{bmatrix} \boldsymbol{x}_{IId}^*(p_a) \\ \boldsymbol{q}_d^*(p_a) \end{bmatrix} \quad \ldots (22)$$

In summary, this approach generates control deflections during a continuation run which correspond to a set or branch of desired steady states. A solution to the bifurcation tailoring problem is not guaranteed in a nonlinear system, especially with hard nonlinearities such as control surface saturation. It is precisely this aspect that allows the open loop bifurcation tailoring to identify the feasibility of proposed closed loop design goals.

5.4 Bifurcation tailoring of the HHIRM

The design goal in this section is to generate a set of equilibria which have zero roll rate p and zero side-slip angle β for the asymmetric fifth order HHIRM. The approach taken is to use

https://doi.org/10.1017/S0001924000001032 Published online by Cambridge University Press

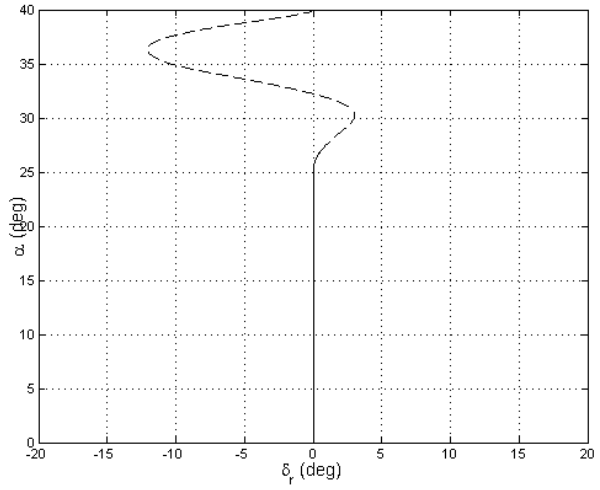


Figure 8. α (deg) *vs* δ_r (deg) for the asymmetric HHIRM tailored to give $\beta = p = 0$.

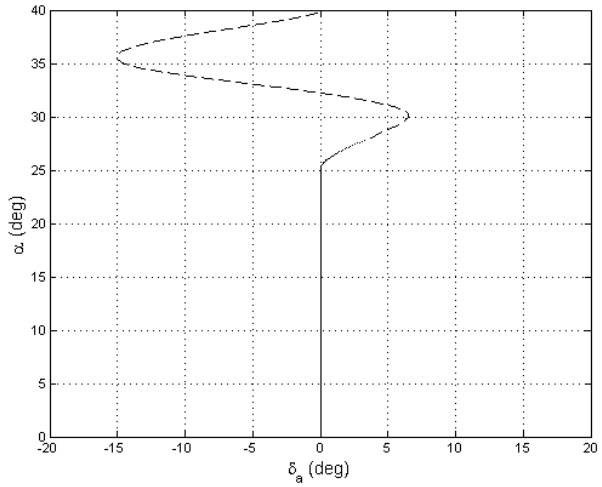


Figure 9. α (deg) *vs* δ_a (deg) for the asymmetric HHIRM tailored to give $\beta = p = 0$.

open loop bifurcation tailoring to achieve step 7 in the CDF; identify if the design goal is physically achievable.

The continuation algorithm was set up to find aileron and rudder deflections that would give zero sideslip β and zero roll rate p. Two systems of equations were used; the first system solved for α, δ_r, δ_a, q and r for the constrained equilibria and the second calculated the system stability using α, β, p, q and r at each steady state identified.

In the constrained system the $\dot{\beta}$ and $\dot{r}$ equations were solved for δ_r and δ_a respectively (for the desired β and p values). For stability, β and p again took their desired (specified) values and perturbations in both were used to find the Jacobian matrix.

The results of the run are shown in Figs 7, 8 and 9. Plots are shown of α against δ_e, δ_r and δ_a. The continuation parameter for the run was the elevator, δ_e, and the limits placed on the run were $0 \le \alpha \le 40$ degrees. The upper limit of 40 degrees was chosen for this run as at just over 40 degrees α both aileron and rudder rapidly saturate. This demonstrates graphically that the desired equilibria are achievable up to the 40 degree α limit.

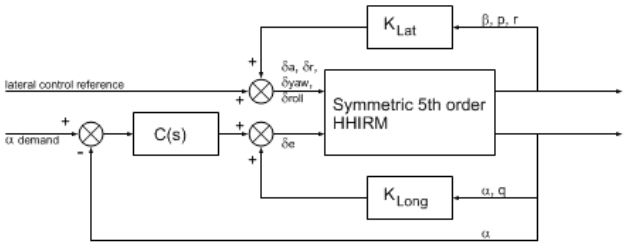


Figure 10. HHIRM control system.

The stability results used for the plot lines in Figs 7, 8 and 9 are based on the the fifth order system with the states α, β, p, q and r. These results indicate a Hopf bifurcation and loss of stability before the complex pair meet on the real axis and the system becomes divergent at high α. The change in stability from the baseline analysis is a result of a change in the phase space through which the system now moves. Hence the stability of the system is different to that of the unaugmented aircraft because the trimmed values of the states are different.

The calculated aileron and rudder deflections (shown in Figs 8 and 9) become non-zero at the point where the asymmetry sets in on the baseline aircraft (i.e. at α = 26 degrees). Thus the steady-state deflections are used to offset the non-zero lateral-directional moments that are contained in the HHIRM model.

These results are not in themselves a usable control scheme, most notably due to the remaining lack of stability and uniqueness that offers little improvement over the baseline aircraft. There are, however, two possible routes to follow; the first is to take the calculated schedules as they stand and to add feedback in order to stabilise the system on the newly created branch.

The second route is to use the results as a guide for an alternative control scheme. It is clear that the model has enough control power to counter the steady state asymmetric moments up to α = 40 degrees. Therefore open loop bifurcation tailoring has confirmed sufficient control authority for steady states and given a useful degree of visibility as to the evolution of the system as parameters vary. Alternative control strategies and stuctures may now be implemented in the knowledge that the control surfaces will not saturate over the specified range.

In this section it has been shown that steps 6 and 7 within the continuation design framework can be carried out using open loop bifurcation tailoring and can be used to investigate possible control system design requirements. The feasibility of defined equilibria have been checked, confirming sufficient steady state control motivation before implementation of the final control scheme.

6.0 CLOSED LOOP HHIRM RESULTS

In Section 5 results were shown for the HHIRM which looked at several steps from section A (Analysis of the baseline model) and B (Define and check feasibility of desired equilibria) in the continuation design framework. In this section results are presented for section C (Design and evaluate gain scheduled controller).

6.1 Desired eigenstructure

The overall design goal for the HHIRM is to create a single branch of stable steady states which exhibit demanded stability modes. For the purposes of this paper, eigenstructure assignment is used to calculate the control system gains and a standard command augmentation system (CAS) is used to create the

https://doi.org/10.1017/S0001924000001032 Published online by Cambridge University Press

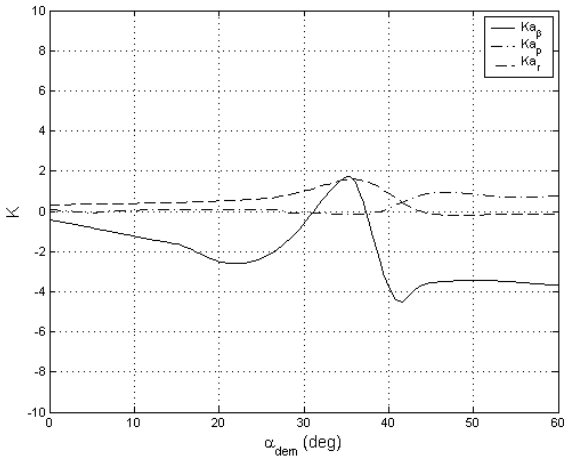


Figure 11. Lateral feedback to δ_a.

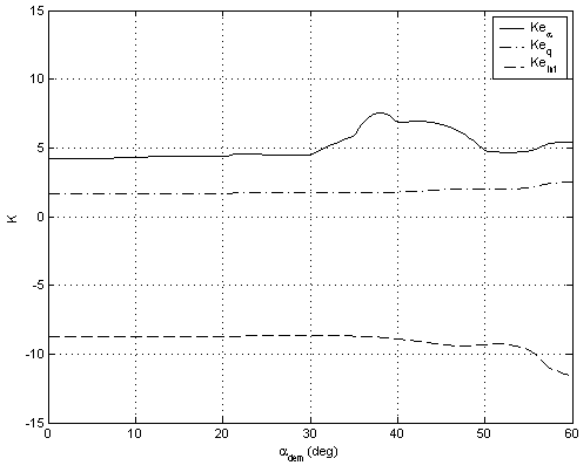


Figure 13. Longitudinal feedback to δ_e.

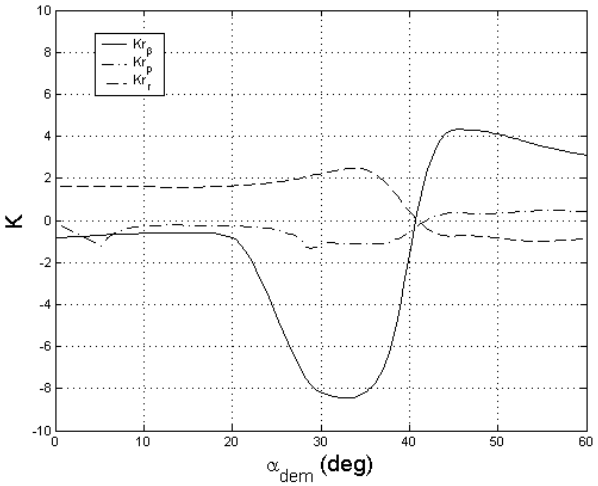


Figure 12. Lateral feedback to δ_r.

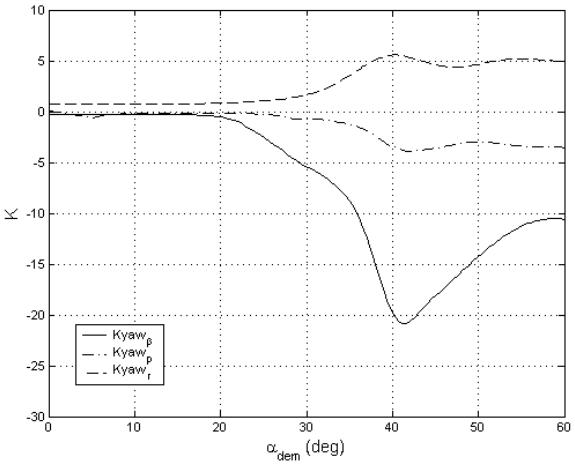


Figure 14. Lateral feedback to δ_{yaw}.

demanded response. The following desired eigenvalues are selected to meet level 1 handling qualities requirements[27]:

Short period	$-2{\cdot}0 \pm 2{\cdot}0j$
Dutch roll	$-1{\cdot}5 \pm 1{\cdot}5j$
Roll subsidence	$-3{\cdot}0$

There are two complex pairs and a single real eigenvalue. The eigenvector selection was made to provide maximum decoupling between longitudinal and lateral modes. Thus, if achievable, the closed loop system should display conventional closed loop aircraft modes.

6.2 Closed loop symmetric HHIRM

The purpose of this section is to demonstrate the benefit of using the continuation design framework to generate gain scheduled controllers. In order to minimise the complexity of the control system the symmetric version of the HHIRM has been implemented which means that for the lateral modes only a stability augmentation system (SAS) is required.

The lateral-directional aerodynamic controls are augmented with thrust vectoring (detailed in Section 4.2) and the throttle has been set to its maximum setting of 1·0. This is done to compensate for the loss in aerodynamic control authority at high α. The augmented system results in increased overall lateral-directional control authority and corresponding smaller required feedback gains.

Figure 10 is a schematic diagram of the lateral SAS and the longitudinal CAS implemented on the symmetric HHIRM. A standard eigenstructure assignment routine is used to place the Dutch roll, roll subsidence, short period and CAS integrator modes. The system is symmetric and decoupled throughout the desired range of $0 \leq \alpha \leq 60$ degrees and therefore only the lateral states are fed back to the lateral control and only the longitudinal controls are fed back to the elevator. There is no need for cross terms in order to decouple the system.

The continuation software AUTO[28] was set up to find the steady states whilst calculating the closed loop feedback gains. This results in the steady states being trim points of the closed loop system and both the controller and the aircraft being trimmed. The steady state gains are stored as gain schedules and are shown in Figs 11-15. These show a smooth variation in all five sets of gains over the required α range.

Figures 11, 12 and 13 show the longitudinal and lateral state feedback gains to the longitudinal (elevator δ_e) and lateral (aileron δ_a and rudder δ_r) aerodynamic control surfaces. The gains are

https://doi.org/10.1017/S0001924000001032 Published online by Cambridge University Press

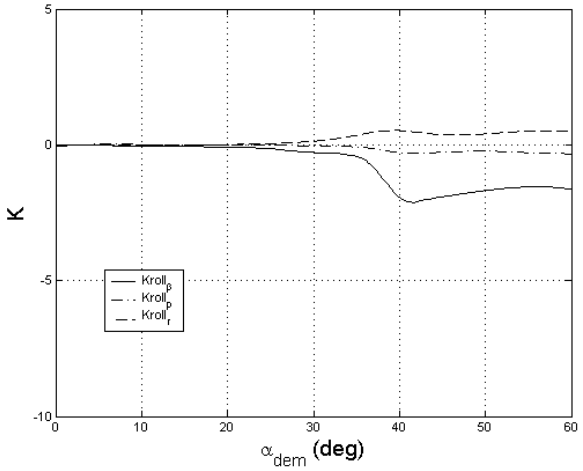


Figure 15. Lateral feedback to δ_{roll}.

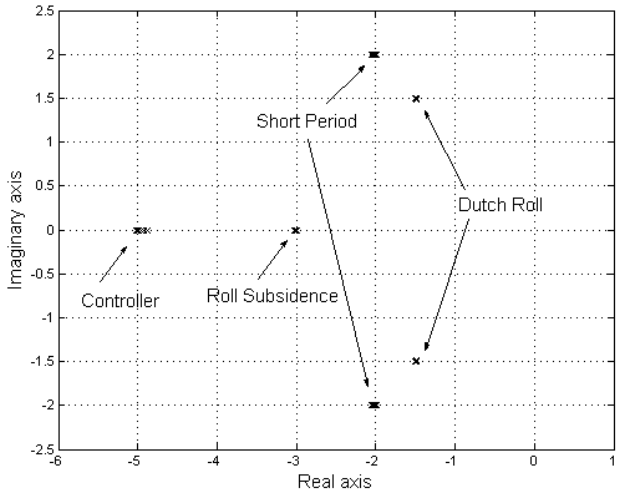


Figure 16. Closed loop eigenvalues.

relatively small and show a smooth variation. In the lateral gains there are sign changes in the gains corresponding to the high α region reflecting the nonlinearities present in the HHIRM model.

What is not shown here in the interests of brevity is that without thrust vectoring the gains ramp up considerably beyond $\alpha \approx 25$ degrees due to the eigenstructure requirements and the loss in aerodynamic control surface effectiveness. This leads to rapid saturation of the control system at high α during simulation.

Figures 14 and 15 show the lateral feedback gain variation to the thrust vectoring nozzles. These gains are small at low α where the aerodynamic control surfaces have sufficient control authority and increase in magnitude at high α in order to compensate for the loss in aerodynamic control.

The maximum gain for the nozzles is found at $\alpha \approx 40$ degrees where the aerodynamic control power is at a minimum. It is interesting to note that unlike the aerodynamic controls there is no reversal in the sign of the gains. This is because the sense of the control remains constant no matter what the angle-of-attack (unlike the aerodynamic control gains shown in Figs 11 and 12).

There are several factors which influence the magnitude of the nozzle control gains including available thrust and demanded eigenvalues. Using the continuation design framework it is possible to schedule available thrust or demanded eigenstructure

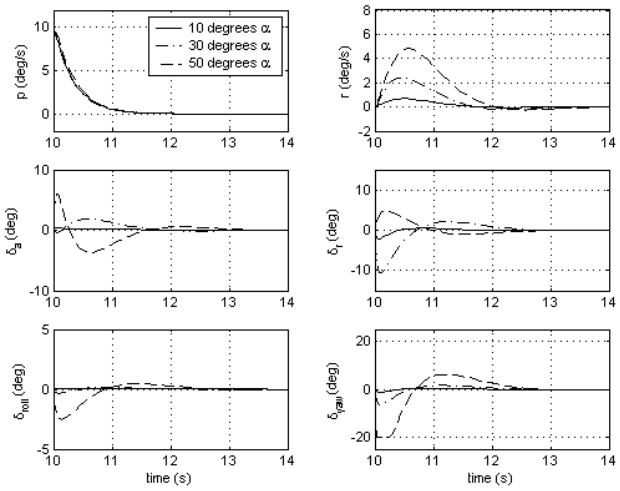


Figure 17. Thrust vectoring HHIRM time simulation: roll response.

with an aircraft state such as angle-of-attack, α. This approach could be taken where insufficient control power were available and reduced dynamic response would be preferable to control surface saturation.

Figure 16 is a plot of the system eigenvalues throughout the demanded α range ($0 \le \alpha \le 60$ degrees). This plot was generated on a second continuation run with the gains scheduled against the continuation parameter (step 10 from the CDF – If necessary re-run the continuation solving for additional branches). No additional branches were identified and it is evident that there is minimal variation in the eigenvalue position due to the smooth variation in required gains. Although simple actuator models were used for both aerodynamic and thrust vectoring controls, only the eigenvalues associated with the Dutch roll, roll subsidence, short period and integrator are shown.

Reaching step 10 in the CDF, this paper has shown an analysis of the baseline HHIRM model, defined and checked the feasibility of the desired equilibria (they already exist in the baseline symmetric HHIRM model) and designed a gain scheduled controller, calculated using an embedded eigenstructure assignment routine within the continuation software.

It is possible to account for some of the hidden coupling terms when scheduling against closely coupled states[19] which is given as step 11 in the CDF. For the purposes of this paper however, the last set of results will be time simulations of the closed loop HHIRM aircraft model with the gains scheduled with the demanded input. Because the closed loop system is fully decoupled and the lateral directional feedback gains are scheduled with α, hidden coupling terms do not present a problem.

Figure 17 shows the response of the closed loop system to a ten degree/s perturbation in roll rate *p*. The first plot shows that for all three values of α (10, 30 and 50 degrees), the roll rate response is almost identical; an exponential first order decay characteristic. This is because the eigenvector requirements were selected to ensure that the Dutch roll mode remained dominant in sideslip, β, and yaw rate, *r*. As a result, perturbations in roll excite the roll subsidence mode no matter where in the a range the system is excited.

Different aileron, rudder and thrust vectoring deflections are required at the different angles-of-attack. There is a small period in which the thrust vectoring yaw control δ_{yaw} saturates. There is no visible effect on the overall response of the aircraft; however, it is a sign that the gains of the system are too high if such a small perturbation in roll rate causes saturation. The roll control

https://doi.org/10.1017/S0001924000001032 Published online by Cambridge University Press

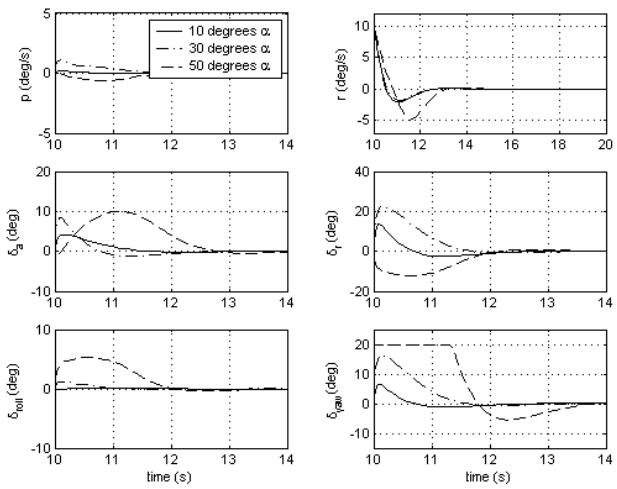


Figure 18. Thrust vectoring HHIRM time simulation: yaw response.

motivators (δ_a and δ_{roll}) only undergo small deflections, indicating sufficient control power whereas both yaw motivators (δ_r and δ_{yaw}) undergo large deflections indicating insufficient δ_{yaw} authority for the required response.

Figure 18 shows the response of the aircraft to a 10 degree/s yaw perturbation applied after 10 seconds. The yaw rate response, r, is clearly second order in nature and for the 10 and 30 degree α plots represents an ideally damped ($\zeta = 0{\cdot}707$) Dutch roll mode. However, at 50 degrees α the response is different. The reason for this becomes obvious if the plot of the thrust vectoring yaw control is considered. Saturation occurs almost immediately after 10 seconds and continues for almost 1·5 seconds. This again shows that there is insufficient yaw control available to give the response required even with the additional thrust vectoring.

As noted before, in order to prevent saturation, the requirements on the eigenstructure assignment could be relaxed. If there were no requirement to keep specific components of a mode consistent throughout the α range then this would result in lower gains but a dynamic response that would vary as α increases. Secondly, the position of the eigenvalues could be relaxed and moved closer to their nominal positions. Finally, limits on the thrust vectoring capability were chosen to be conservative. If more thrust were available, maximum nozzle deflection and/or the distance between the nozzles increased then the gains required would correspondingly decrease.

At this point, step 12 in the continution design framework (time simulations) has highlighted several changes that could be made to the desired dynamic response and control system. If this control system design were to be used in practice then iterating through the CDF would allow the control system design to be refined.

7.0 CONCLUSIONS

This paper has introduced the concept of embedding a controller design method within a continuation algorithm. This allows gain schedules to be defined over wide operating regions of smooth nonlinear dynamical systems. Eigenstructure assignment was used as an example to design gain schedules that – within the limits of available control power – maintain consistent handling qualities over a very large incidence range for a fifth order implementation of a hypothetical aircraft model with highly nonlinear aerodynamics.

The continuation design framework (CDF) represents the extension of bifurcation and continuation methods from an assessment tool to a systematic methodology for control law design. A particular strength of the technique is the link with the underlying physics of the problem, allowing the designer to easily identify design goals, implement controllers and evaluate changes to the baseline model.

ACKNOWLEDGEMENTS

The authors are grateful for the provision of the HHIRM model by QinetiQ, Bedford.

REFERENCES

1. MEHRA, R.K., KESSEL, W.C. and CARROLL, J.V. Global stability and control analysis of aircraft at high angles of attack 1977, Technical Report ONR-CR215-248-1, US Office of Naval Research.
2. MEHRA, R.K. and CARROLL, J.V. Global stability and control analysis of aircraft at high angles of attack, 1978, Technical Report ONR-CR215-248-2, US Office of Naval Research.
3. MEHRA, R.K. and CARROLL, J.V. Global stability and control analysis of aircraft at high angles of attack, 1979, Technical Report ONR-CR215-248-3, US Office of Naval Research.
4. JAHNKE, C.C. and CHEN, G. Nonlinear stability analysis of steady states, 1995, Proceedings of AIAA Atmospheric Flight Mechanics Conference, AIAA-95-3449.
5. JAHNKE, C.C. and CULICK, F.E.C. Application of bifurcation theory to the high-angle-of-attack dynamics of the F-14. *J Aircr*, 1994, **31**, pp 26-34.
6. GUICHETEAU, P. Non-linear flight dynamics, 1993, AGARD lecture series 191.
7. PLANEAUX, J.B. and MCDONNELL, R.J. Thrust contributions to the spin characteristics of a model fighter aircraft, 1991, AIAA-91-2887.
8. LOWENBERG, M.H. Application of Bifurcation Analysis to Multiple Attractor Flight Dynamics, 1998, PhD thesis, University of Bristol.
9. LOWENBERG, M.H. Bifurcation analysis of multiple-attractor flight dynamics. *Phil Trans Royal Society London A*, 1998, **356**, pp 2297-2319.
10. LOWENBERG, M.H. Development of control strategies to modify spin behaviour, 1998, Proceeedings of AIAA Atmospheric Flight Mechanics Conference, AIAA-98-4267.
11. LOWENBERG, M.H. and RICHARDSON, T.S. The continuation design framework for nonlinear aircraft control, 2001, Proceedings of AIAA Guidance, Navigation and Control Conference, AIAA-2001-4100.
12. GIBSON, L., NICHOLS, N.K. and LITTLEBOY, D.M. Closed loop design for a simple nonlinear aircraft model using eigenstructure assignment, 1997, Proceedings of AIAA Guidance, Navigation and Control Conference, AIAA-97-3779.
13. LITTLEBOY, D.M. and SMITH, P.R. Using bifurcation methods to aid nonlinear dynamic inversion control law design, *J Guidance, Control and Navigation*, 1998, **21**, (4), pp 632-638.
14. GOMAN, M.G. and KHRAMTSOVSKY. Application of continuation and bifurcation methods to the design of control systems. *Phil Trans Royal Society London A*, **356**, (1745) 1998, pp 2277-2295.
15. GOMAN, M.G., ZAGAINOV, G.I. and KHRAMTSOVSKY, A.V. Application of bifurcation methods to nonlinear flight dynamics problems. *Prog Aerospace Sci*, 1997, **33**, pp 539-586.
16. GOMAN, M.C. and KHRAMTSOVSKY. Global stability analysis of nonlinear aircraft dynamics, 1996, AIAA-97-3721.
17. NELSON, R.C. *Flight Stability and Automatic Control*, 1998, McGraw-Hill.
18. DORSETT, K.M. and MEHL, D.R. Innovative control effectors (ICE), January 1996, Wright Laboratories, Wright-Patterson AFB, OH, WL-TR-96-3043.
19. LOWENBERG, M., RICHARDSON, T., DAVISON, P. and DI BERNARDO, M. Control of nonlinear aircraft models using dynamic state-feedback gain scheduling, 2003, Proceedings of AIAA Guidnace, Navigation and Control Conference, AIAA-2003-5503.
20. LOWENBERG, M.H., JONES, C.D.C. and RICHARDSON, T.S. Dynamic state-feedback gain-scheduled control of the ICE 101-TV, 2004, Proceedings of AIAA Guidance, Navigation and Control Conference, AIAA-2004-4754.

https://doi.org/10.1017/S0001924000001032 Published online by Cambridge University Press

21. GUCKENHEIMER, J. and HOLMES, P. *Nonlinear Oscillations, Dynamical Systems, and Bifurcations of Vector Fields*, 1983, Springer.
22. TEUKOLSKY, S.A., PRESS, W.H., FLANNERY, B.P. and VETTERLING, W.T. *Numerical Recipes: Fortran Example Book*, 1993, Cambridge University Press.
23. SEYDEL, R. *Practical Bifurcation and Stability Analysis: From Equilibrium to Chaos. Interdisciplinary Applied Mathematics*, 1994, Springer-Verlag.
24. GOMAN, M.G., KHRAMTSOVSKY, A.V. and USOLTEV, S. High incidence aerodynamics model for hypothetical aircraft, 1995, Technical Report 15/5DRA, TsAGI.
25. WILSON, R.J., FLICK, B.C., BOWERS, A.H., PAHLE, J.W. and ROOD, R.L. An overview of the NASA F-18 high alpha research vehicle, 1996, Technical report, NASA Technical Memorandum 4772.
26. LOWENBERG, M., STOTEN, D., WANG, X., CHARLES, G. and DI BERNARDO, M. Bifurcation tailoring of equilibria: a feedback control approach, Special Issue on Control of Bifurcations, *Latin American J Applied Research*, 2001, **31**.
27. HODGKINSON, J. *Aircraft Handling Qualities*, 1999, American Institute of Aeronautics and Astronautics Press.
28. DOEDEL, E.J. and WANG, X.J. AUTO94: Software for continuation and bifurcation problems in ordinary differential equations, 1995, Technical Report CRPC-95-2, California Institute of Technology.

https://doi.org/10.1017/S0001924000001032 Published online by Cambridge University Press